

for F values of 5997 reflections with $F_o^2 > 2\sigma(F_o^2)$, $S = 1.215$ for 689 parameters. Residual electron density extremes were 0.955 and $-1.662 \text{ e } \text{\AA}^{-3}$. Crystallographic data (excluding structure factors) for the structures reported in this paper have been deposited with the Cambridge Crystallographic Data Centre as supplementary publication no. CCDC-147870 ($[\text{Zn}\{(E,E)\text{-1}\}](\text{ClO}_4)_2$), CCDC-152441 ($[\text{Cu}\{(E,E)\text{-1}\}](\text{ClO}_4)_2$), and CCDC-152442 ($[\text{Co}\{(E,E)\text{-1}\}]\text{I}_2$). Copies of the data can be obtained free of charge on application to CCDC, 12 Union Road, Cambridge CB21EZ, UK (fax: (+44)1223-336-033; e-mail: deposit@ccdc.cam.ac.uk).

- [23] The yields listed in Scheme 2 are yields after chromatography or recrystallization. Sometimes the mixture of olefin diastereomers complicates purification and, in particular, is a factor in the modest yields of $[\text{Co1}]\text{L}_2$ and $[\text{Ni1}]\text{L}_2$. The very low yield of $[\text{Hg1}]\text{L}_2$ by route (a) is caused by the lability of the ligands in the precursor complex $[\text{Hg2}]\text{L}_2$, which liberates free amine or imine in the reaction and prevents RCM occurring. All compounds gave satisfactory mass spectra, elemental analysis, IR, UV/Vis, and, with the exception of the paramagnetic catenates, ^{13}C and ^1H NMR data.
- [24] S. Jurisson, D. Berning, W. Jia, D. Ma, *Chem. Rev.* **1993**, 93, 1137–1156.
- [25] D. Parker, *Chem. Br.* **1994**, 818–822.
- [26] G. J. P. Britovsek, V. C. Gibson, D. F. Wass, *Angew. Chem.* **1999**, 111, 448–468; *Angew. Chem. Int. Ed.* **1999**, 38, 428–447.
- [27] L. Douce, A. El-Ghayoury, A. Skoulios, R. Ziessel, *Chem. Commun.* **1999**, 2033–2034.

Insertion of Helium and Molecular Hydrogen Through the Orifice of an Open Fullerene**

Yves Rubin,* Thibaut Jarrosson, Guan-Wu Wang, Michael D. Bartberger, K. N. Houk,* Georg Schick, Martin Saunders,* and R. James Cross*

*Dedicated to Professor Fred Wudl
on the occasion of his 60th birthday*

One of the most exciting features of C_{60} and the higher fullerenes is that their carbon cages have inner cavities large enough to hold any atom and even small molecules.^[1, 2] The physical and chemical properties of these caged compounds (endohedral complexes) are determined by the degree of interaction established with the π -electron shell and the overall oxidation state of the complex.^[3] As such, endohedral

complexes offer a number of prospects for novel materials.^[4–6] A large effort has been invested in finding efficient methods for the preparation and purification of these compounds.^[1, 2, 7] So far, endohedral complexes have been formed with lanthanide or alkaline earth metals as charge transfer species,^[1, 2] and with the rare gases^[8, 9] or atomic nitrogen^[10] as neutral complexes. Processes using the evaporation of graphite–metal oxide composites, as well as high-pressure and high-temperature or even high-energy plasma insertions into pure fullerenes, have been reported.^[1–7] These methods constitute remarkable achievements and have already brought forth important insight into the properties of endohedral fullerene complexes. Nevertheless, they are still limited in scope and, more significantly, tend to give small amounts of material or meager incorporation fractions.

A stimulating prospect for the formation of these compounds can be described as a “molecular surgery” approach, which consists of the chemical creation of an opening within the fullerene cage (Figure 1a).^[4] The opened species would allow the introduction of an atomic or molecular species, which could be followed by the “suturing” of broken bonds back onto the original framework. Each of these steps presents unique nontrivial challenges. The development of an effective method to open up the framework of C_{60} by a one-pot reaction with bisazide **2**, to afford bislactam **1**,^[11] provides an unprecedented opportunity for the preparation of endohedral complexes. We now report the successful insertion of two small neutral gases, helium and molecular hydrogen, into the fullerene bislactam derivative **1** which results in the highest incorporation fractions for any gas to date in a direct insertion process.

Bislactam **1** has currently the largest orifice formed in the shell of a fullerene with an inviting open-mouth shape.^[4, 11] The amount of energy needed to push atoms or molecules through the orifice of **1** was first calculated using hybrid density functional theory. Activation barriers to insertion obtained as a function of guest size are listed in Table 1. The ground-state structures for empty bislactam **1**, its inclusion complexes of the inert gases He, H_2 , Ne, N_2 , and Ar, and the transition structures for their encapsulation were fully optimized at the B3LYP/3-21G level of theory, and energies were computed from these geometries using the 6-31G** basis set.^[12]

The overall insertion processes for the smallest species (He, H_2) are predicted to be slightly endothermic (0.2 – $1.4 \text{ kcal mol}^{-1}$, Table 1). Patchkovskii and Thiel have investigated the encapsulation of helium by C_{60} using MP2 calculations,^[13] and found a favorable binding of $2.0 \text{ kcal mol}^{-1}$ as a result of van der Waals interactions of all sixty carbon atoms with the helium atom. These authors conclude that DFT calculations underestimate the exothermicity of He encapsulation within C_{60} by about 3 kcal mol^{-1} compared to the MP2 results, and thus the encapsulation of H_2 and He within the fullerene framework of **1** can be expected to be thermoneutral or slightly exothermic.

The predicted barrier for insertion of H_2 is nearly double that of helium, even though both species have similar van der Waals radii (1.20 and 1.22 \AA , respectively).^[14] The single imaginary vibrational modes at the transition states for

[*] Prof. Y. Rubin, Prof. K. N. Houk, T. Jarrosson, Dr. M. D. Bartberger, Dr. G. Schick
Department of Chemistry and Biochemistry
University of California, Los Angeles
Los Angeles, CA 90095-1569 (USA)
Fax: (+1) 310-206-7649
E-mail: rubin@chem.ucla.edu, houk@chem.ucla.edu
Prof. M. Saunders, Prof. R. J. Cross, Dr. G.-W. Wang^[+]
Department of Chemistry
Yale University
New Haven, CT 06520 (USA)
Fax: (+1) 203-432-6144
E-mail: ms@gaus90.chem.yale.edu, james.cross@yale.edu

[+] Present address: Department of Chemistry
University of Science and Technology of China
Hefei, Anhui 230026 (PR China)

[**] This work was supported by grants from the National Science Foundation.

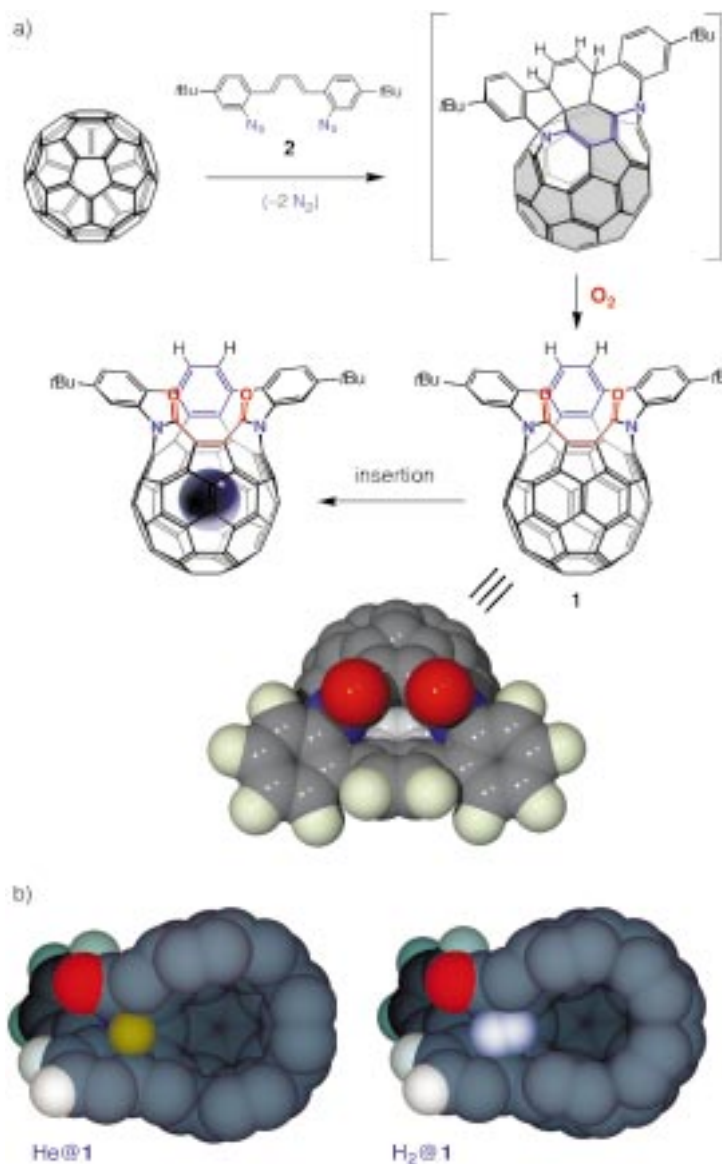


Figure 1. a) Preparation and structure of bislactam **1** and insertion of He and H₂ in this molecular container. The synthesis of the open fullerene **1** from bisazide **2** was previously reported.^[11] b) Cutout views of space-filling models for the B3LYP/3-21G transition structures of both helium and molecular hydrogen insertions.

Table 1. Predicted activation barriers for insertion and cage escape, and energies (B3LYP/6-31G**//B3LYP/3-21G, kcal mol⁻¹) of encapsulation for the neutral guests He, Ne, H₂, N₂, and Ar gases inside the open fullerene bislactam **1**. Insertion temperatures are estimated as explained in the text.

Guest	Volume ^[22] [Å ³]	Est. insertion temperature [°C]	Barrier to insertion	Energy of encapsulation	Barrier to escape
He	11.0	124	+24.5	+0.2	+24.3
H ₂	19.0	397	+41.4	+1.4	+40.0
Ne	14.6	384	+40.6	-1.1	+41.7
N ₂	35.3	1550	+112.4	+5.6	+106.8
Ar	28.9	1930	+136.3	+6.1	+130.2

He or H₂ insertions (255i and 502i cm⁻¹, respectively) clearly correspond with the exit/entrance motion of He or H₂. The fullerene cage itself undergoes practically no distortion in this

process, except for a comparatively low amplitude, strain-releasing vibration of the C=C bond between the two carbonyl groups.

The difference in barriers can be understood in terms of the varying amounts of constriction both species encounter at their respective transition states to insertion and escape (Figure 1b). With its elongated shape and larger surface area, H₂ experiences much greater steric interaction while forcing its way through the “neck” of bislactam **1**, while the spherical helium atom encounters much less surface contact. There is a roughly linear correlation between the guest volumes (He and N₂) and activation barriers for insertion (Table 1). The total surface exposed to the long narrow channel, not the shortest distance across the guest molecule, determines the barrier.

The temperatures required for guest insertion were estimated from the computed activation barriers (Table 1). These values were obtained from the Arrhenius equation using an approximated pre-exponential factor^[15] and an arbitrary 24 h reaction period. These estimates show that helium should insert relatively easily at temperatures around 100–120 °C, while H₂ would require much more drastic conditions, with temperatures of about 400 °C being necessary to effect insertion.

Besides overcoming such insertion barriers, the reaction equilibria can be assumed to lie in a thermoneutral to slightly exothermic range, as discussed earlier. However, the entropic cost for the insertion process is very high (see below). The occupied fraction of the gas at atmospheric pressure under equilibrium conditions might be expected to be small because of the small volume of the cavity. Higher pressures would therefore enhance the fraction of gas incorporated.

Incorporation experiments were initially carried out with helium. The ³He isotope constitutes a very convenient and sensitive NMR probe for environmental changes;^[9] it displays large upfield chemical shifts on insertion ($\delta = -6.3$ for ³He@C₆₀ to -28.8 for ³He@C₇₀), and does not give the same interference problems that impurities can introduce in ¹H NMR spectroscopy. Incorporation was found to occur readily, even under low helium pressure (3–4 atm, 100 °C, 8 h) using a sealed NMR tube. ³He NMR (deuterated *ortho*-dichlorobenzene ([D₄]ODCB), 31268 accumulated transients) showed a new peak at $\delta = -10.10$ relative to the reference at $\delta = 0$ for the free dissolved ³He gas. The fraction incorporated at this low pressure (0.03 %, or 0.05 % after 24 h under the same conditions) already approaches that of ³He@C₆₀ (0.1 %) prepared by the direct high pressure method.^[8, 9] The helium can be ejected by heating above 150 °C. Higher pressures were used subsequently to increase the fraction of helium inside bislactam **1**: Heating compound **1** as a crystalline powder under a helium atmosphere contained within a crimped copper tube (288–305 °C, ca. 475 atm (ca. 7000 psi) 7.5 h) in a high-pressure vessel, afforded ³He@**1** with about 1.5 % molar ratio of the gas versus a ³He@C₆₀ standard. Such high incorporation allowed for the direct experimental determination of the activation barrier for escape of ³He (Table 2, Figure 2). The change in the relative ³He signal intensities collected at four constant temperatures (80, 100, 120, and 130 °C) versus ³He@C₆₀ as the nondecomplexable standard were monitored over time

Table 2. Experimental data for the release of ^3He from bislactam **1** at four temperatures, integrated changes in ratios of $^3\text{He@1}$ to $^3\text{He@C}_{60}$, and rates of release.

T [°C]	t [h]	$^3\text{He@1}/^3\text{He@C}_{60}$	k [s ⁻¹] ($\times 10^6$)
80 \pm 2	24	7.62 \rightarrow 6.45	1.9
100 \pm 1	12	6.45 \rightarrow 3.39	14.9
120 \pm 1	3	3.39 \rightarrow 1.47	77.4
130 \pm 0.5	1	1.47 \rightarrow 0.86	148.9

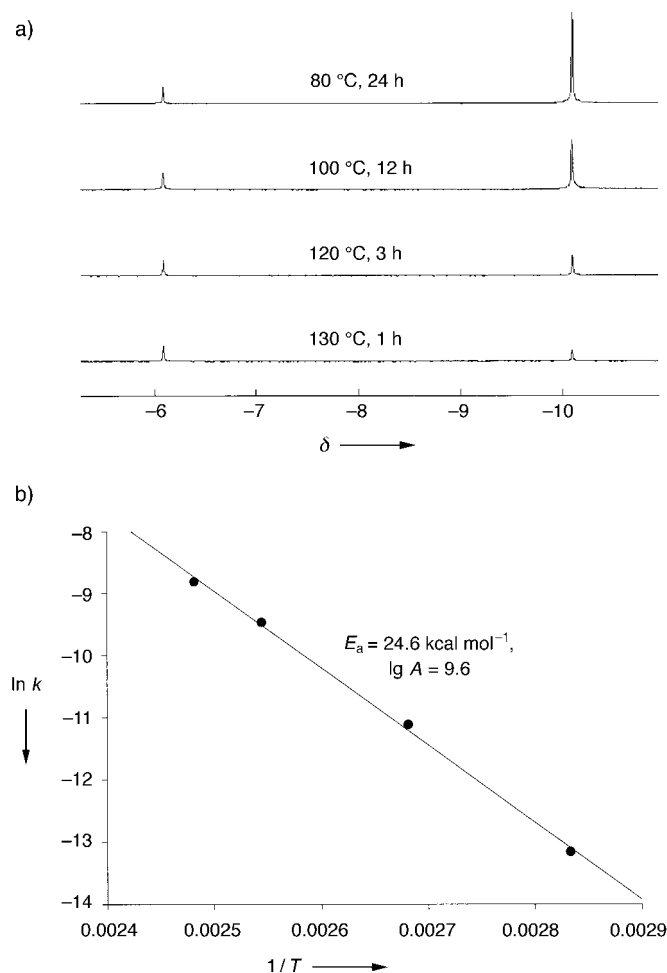


Figure 2. a) ^3He NMR spectra of $^3\text{He@C}_{60}$ ($\delta = -6.09$) and $^3\text{He@1}$ ($\delta = -10.10$) at four release temperatures. The ratios of both helium-containing compounds were compared by integration. b) Arrhenius plot for the release of helium from **1**.

(Figure 2a), with the resulting Arrhenius plot giving the excellent linear fit shown in Figure 2b. The activation barrier for escape of ^3He from the cage is $24.6 \pm 0.8 \text{ kcal mol}^{-1}$, which is in excellent agreement with the calculated value (Table 1).

The Arrhenius preexponential factor ($10^{9.6}$) corresponds to a substantially unfavorable entropy of activation ($\Delta S^\ddagger \cong -17 \text{ eu}$). Vibrational analysis of the transition structure for helium release clearly demonstrates the loss of translational degrees of freedom of the helium atom upon reaching the constrictive neck of the orifice of bislactam **1** (Figure 1b). However, when fully encapsulated within **1**, the helium atom does not significantly interact with the inner walls of the fullerene cage nor the gate orifice. The resulting practically

free motion of ^3He encapsulated in **1** is lost in the transition state for cage escape as a consequence of the constriction at the orifice. Consideration of the release of helium from the fullerene cage of **1** as a quasi-bimolecular reaction possessing a constricted transition state, rather than as a unimolecular reaction, explains the observed low pre-exponential factor and negative activation entropy. The entropy of ^3He , all translational, is 30 eu. The maximum ΔS^\ddagger value for completely restricting the translational motion of a free helium atom would thus be -30 eu , but the measured activation entropy of helium release is more than one half this value.

The incorporation of molecular hydrogen was investigated in the same manner. As expected from the calculations, the incorporation of H_2 required much more forcing conditions for insertion than helium. After several unsuccessful trials in high-boiling solvents, bislactam **1** was heated as a crystalline powder up to the limit of decomposition (400°C ,^[16] 48 h, $\leq 30\%$ of decomposed material) in a standard autoclave under 100 atm (1500 psi) of hydrogen. Purification by column chromatography (SiO_2 , toluene/EtOAc 9/1) was performed to give pure bislactam **1** together with the fraction of incorporated material $\text{H}_2\text{@1}$. The ^1H NMR spectrum showed a new peak at $\delta = -5.43$, in addition to the expected aromatic and aliphatic resonances for the bislactam moiety (Figure 3). This

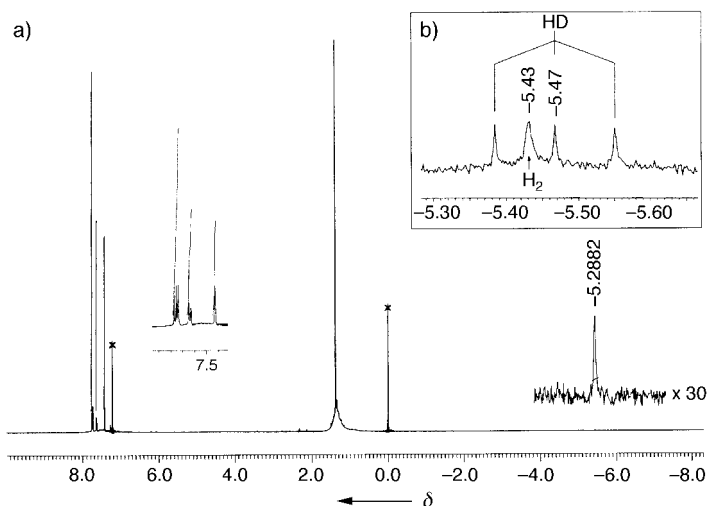


Figure 3. a) ^1H NMR spectrum of the H_2 -incorporated material. The signal corresponding to $\text{H}_2\text{@1}$ at $\delta = -5.43$ (HD@1: $\delta = -5.47$ in inset) has approximately 5% integral intensity of the aromatic signals for the empty and filled species.^[18] The reasons for the broad aromatic and *tert*-butyl peaks are not quite clear, but they also appear similarly broadened in the pristine bislactam **1** and are most likely post-purification oxidation byproducts (bislactam **1** is somewhat unstable in solution). b) ^1H NMR spectrum of the HD-incorporated material; the sample contained about 30% of H_2 as an impurity generated during the preparation of the gas from CaH_2 and D_2O .

new peak is shifted by 10 ppm upfield from dissolved H_2 ($\delta = 4.53$), measured separately, clearly lying outside the normal resonance range ($\delta = 0\text{--}10$) of most proton-containing compounds.^[17] The relative intensity for incorporated H_2 was found to be as high as 5%.^[18] This is by far the highest amount of direct incorporation in a fullerene obtained for any gas,

which bodes well for future insertions of higher fractions of these gases under extreme pressures.

A fully convincing demonstration of this incorporation was obtained by replacing H₂ with the monodeuterated species HD (309–322 °C, 15 h, 340 atm (5000 psi)).^[19] The corresponding resonance at $\delta = -5.47$ is now a triplet with a coupling constant of 41.8 Hz (Figure 3, inset), which is in accord with the literature value.^[20] Interestingly, the peak for the H₂ signal, which originated as an impurity during the synthesis of HD from CaH₂ and D₂O, appears as a much broader line than the other three HD signals. A likely explanation for this effect is that the very short bond length in the H–H molecule results in a strong dipole–dipole interaction between the two nuclei which leads to rapid relaxation and broadening since its rotation is somewhat impeded by the cage.

Comparison of the experimental chemical shifts observed for H₂ and ³He inside bislactam **1** and their calculated values gives further support to the effectiveness of these insertion experiments. ¹H and ³He NMR chemical shifts were calculated at the B3LYP/6-31G** level of theory using the Gauge Invariant Atomic Orbital (GIAO) approach.^[21] The calculated chemical shifts of He and H₂ are predicted to be strongly shielded by the fullerene π -electron shell of **1** as a result of encapsulation and shift substantially upfield (–8.6 and –8.0 ppm, respectively) versus free ³He and H₂; the experimental shielding values are $\delta = -10.10$ and -9.96 , respectively.

The successful incorporation of two gases inside bislactam **1** presages the insertion of metal ions and somewhat larger molecular species within wider openings of future fullerene derivatives.^[4] Furthermore, neon should also insert into bislactam **1** (Table 1), but this element lacks the convenience of having an NMR-active nucleus. On the other hand, the larger neutral gases N₂ and Ar cannot be incorporated within **1** under similar conditions because of the huge associated activation barriers. The important step of closing back the fullerene framework also needs to be studied. We have observed strong peak intensities from C₆₀ cations (up to 35 % (relative intensity) for the peak at $m/z = 720$ amu) being formed in the fast atom bombardment (FAB) mass spectra of bislactam **1**. This result shows that this heavily modified framework can still find its way back to the highly stable fullerene framework of C₆₀. This work shows more generally that open fullerenes afford an opportunity to study the dynamics of passage of small molecules or ions through restricted channels in chemically well-defined systems.

Received: January 8, 2001 [Z16381]

[1] H. Shinohara, *Rep. Prog. Phys.* **2000**, 63, 843–892.

[2] S. Nagase, K. Kobayashi, T. Akasaka, *Bull. Chem. Soc. Jpn.* **1996**, 69, 2131–2142.

[3] T. Akasaka, T. Wakahara, S. Nagase, K. Kobayashi, M. Waelchli, K. Yamamoto, M. Kondo, S. Shirakura, S. Okubo, Y. Maeda, T. Kato, M.

Kako, Y. Nakadaira, R. Nagahata, X. Gao, E. Van Caemelbecke, K. M. Kadish, *J. Am. Chem. Soc.* **2000**, 122, 9316–9317.

[4] Y. Rubin, *Top. Curr. Chem.* **1999**, 199, 67–91, and references therein.

[5] M. S. Dresselhaus, G. Dresselhaus, P. C. Eklund, *Science of Fullerenes and Carbon Nanotubes*, Academic Press, New York, **1996**.

[6] L. J. Wilson, D. W. Cagle, T. P. Thrash, S. J. Kennel, S. Mirzadeh, J. M. Alford, G. J. Ehrhardt, *Coord. Chem. Rev.* **1999**, 192, 199–207.

[7] S. Stevenson, G. Rice, T. Glass, K. Harich, F. Cromer, M. R. Jordan, J. Craft, E. Hadju, R. Bible, M. M. Olmstead, K. Maitra, A. J. Fisher, A. L. Balch, H. C. Dorn, *Nature* **1999**, 401, 55–57.

[8] M. Saunders, R. J. Cross, H. A. Jiménez-Vázquez, R. Shimshi, A. Khong, *Science* **1996**, 271, 1693–1697.

[9] M. Saunders, H. A. Jiménez-Vázquez, R. J. Cross, S. Mroczkowski, D. I. Freedberg, F. A. L. Anet, *Nature* **1994**, 367, 256–258.

[10] A. Weidinger, M. Waiblinger, B. Pietzak, T. A. Murphy, *Appl. Phys. A* **1998**, 66, 287–292.

[11] G. Schick, T. Jarrosson, Y. Rubin, *Angew. Chem.* **1999**, 111, 2508–2512; *Angew. Chem. Int. Ed.* **1999**, 38, 2360–2363.

[12] All calculations were performed with the Gaussian98 program: Gaussian98, Revision A.7, M. J. Frisch, G. W. Trucks, H. B. Schlegel, G. E. Scuseria, M. A. Robb, J. R. Cheeseman, V. G. Zakrzewski, J. A. Montgomery, Jr., R. E. Stratmann, J. C. Burant, S. Dapprich, J. M. Millam, A. D. Daniels, K. N. Kudin, M. C. Strain, O. Farkas, J. Tomasi, V. Barone, M. Cossi, R. Cammi, B. Mennucci, C. Pomelli, C. Adamo, S. Clifford, J. Ochterski, G. A. Petersson, P. Y. Ayala, Q. Cui, K. Morokuma, D. K. Malick, A. D. Rabuck, K. Raghavachari, J. B. Foresman, J. Cioslowski, J. V. Ortiz, A. G. Baboul, B. B. Stefanov, G. Lui, A. Liashenko, P. Piskorz, I. Komaromi, R. Gomperts, R. L. Martin, D. J. Fox, T. Keith, M. A. Al-Laham, C. Y. Peng, A. Nanayakkara, C. Gonzalez, M. Challacombe, P. M. W. Gill, B. G. Johnson, W. Chen, M. W. Wong, J. L. Andres, M. Head-Gordon, E. S. Replogle, J. A. Pople, Gaussian, Inc., Pittsburgh, PA, **1998**.

[13] S. Patchkovskii, W. Thiel, *J. Chem. Phys.* **1997**, 106, 1796–1799.

[14] J. A. Dean, *Lange's Handbook of Chemistry*, 13th ed., McGraw-Hill, New York, **1985**.

[15] A pre-exponential factor for insertion ($A = 10^{8.5}$) was initially estimated by dividing the standard bimolecular factor ($A = 10^{10.5 \pm 0.5}$, see S. W. Benson, *Thermochemical Kinetics*, Wiley, New York, **1976**, p. 156) by a factor of about 100, which reflects the probability factor for the gas to find the approximate 5.5 Å² orifice of bislactam **1** (the van der Waals radius of He is equal to 1.2 Å, thus its cross-section is 4.5 Å²) over its much larger 550 Å² overall external surface (the Connolly molecular area of **1** was determined using Chem3D, Cambridge Scientific, Cambridge, MA 02139).

[16] The temperature was measured with an external thermocouple and is uncalibrated.

[17] A large frequency range (26300 Hz) was chosen to avoid fold-over peaks.

[18] The molar ratio was obtained from averaged integral intensities between the signal at $\delta = -5.43$ and the aromatic protons of bislactam **1**.

[19] HD was prepared by treatment of CaH₂ with D₂O. The fraction of H₂ impurity also formed arises during this reaction from the HDO impurity present in D₂O as verified by ¹H NMR spectroscopy on the dissolved gas (C₆D₆).

[20] P. A. Maltby, M. Schlaf, M. Steinbeck, A. J. Lough, R. H. Morris, W. T. Klooster, T. F. Koetzle, R. C. Srivastava, *J. Am. Chem. Soc.* **1996**, 118, 5396–5407.

[21] For a comprehensive review of the quantum mechanical determination of NMR chemical shifts, see T. Helgaker, M. Jaszunski, K. Ruud, *Chem. Rev.* **1999**, 99, 293–352.

[22] Guest molecular volumes were determined by Monte Carlo integration within an electron density contour of 0.001 electrons Bohr⁻³, as implemented in Gaussian 98. These volume calculations utilized the B3LYP/6-31G** computed density.